Minimum wood density of conifer species portrays changes in spring precipitation at dry and cold Eurasian sites from the forest-steppe and Mediterranean biomes

J. Julio Camarero[1]*, Laura Fernández-Pérez[2], Alexander V. Kirdyanov[3,4], Tatiana A. Shestakova[5], Anastasia A. Knorre[6], Vladimir V. Kukarskih[7] and Jordi Voltas[8]

[1]Instituto Pirenaico de Ecología (IPE-CSIC), Avda. Montañana 1005, E-50059 Zaragoza, Spain
[2]Forest Ecology and Restoration Group, Department of Life Sciences, University of Alcalá, E-28802 Alcalá de Henares (Madrid), Spain
[3]Sukachev Institute of Forest SB RAS, Akademgorodok 50/28, 660036 Krasnoyarsk, Russia
[4]Institute of Ecology and Geography, Siberian Federal University, pr. Svobodny 82, 660041, Krasnoyarsk, Russia
[5]Department of Evolutionary Biology, Ecology and Environmental Sciences, University of Barcelona, 08028 Barcelona, Spain
[6]Department of Forestry, Siberian Federal University, 660041 Krasnoyarsk, Russia
[7]Institute of Plant and Animal Ecology SD RAS, 8 Marta Str. 202, Yekaterinburg, 620144, Russia
[8]Department of Crop and Forest Sciences-AGROTECNIO Center, Universitat de Lleida, Rovira Roure 191, E 25198 Lleida, Spain

*Corresponding author:

J. Julio Camarero

Instituto Pirenaico de Ecología (IPE-CSIC)

Avda. Montañana 1005

50059 Zaragoza, Spain.
E-mail: jjcamarero@ipe.csic.es

Summary

In conifers tracheids fulfill most of the main wood functions (mechanical support, water transport). Earlywood tracheids account for most hydraulic conductivity within the annual tree ring. Therefore, dry conditions during the early growing season, when earlywood is formed, should lead to the formation of narrow tracheid lumens and a dense earlywood. Here we test if there is an inverse relationship between minimum wood density and early growing-season (spring) precipitation. We study growth and density data of three Pinaceae species (*Pinus sylvestris*, *Pinus nigra*, and *Larix sibirica*) widely distributed in three cool-dry Eurasian regions from the forest-steppe (Russia, Mongolia) and Mediterranean (Spain) biomes. Using dendrochronology, we measured for each annual tree ring and the common 1950-2002 period the following variables: earlywood (EW hereafter) and latewood widths (LW hereafter), and minimum (MN hereafter) and maximum wood density (MX hereafter). As expected, dry early-growing season (spring) conditions were associated to low EW values but, most importantly, to high MN values in the three study species. The associations between MN and spring precipitation were stronger than those observed with EW. We interpret the relationship between spring water availability and high minimum density as a drought-induced reduction in lumen diameter, hydraulic conductivity and growth. Consequently, forecasted growing-season drier conditions would translate into increased minimum wood density and reflect a reduction in hydraulic conductivity, radial growth and wood formation. Increased aridity would diminish the ability of Eurasian conifer forests subjected to coldness and drought to fix and store carbon as durable woody pools.

Key words: Black pine, dendroecology, densitometry, Scots pine, Siberian larch, water availability, wood density.

Introduction

Wood fulfils provides to trees: mechanical support, transport, storage and defence against biotic agents (Zobel and van Buijtenen, 1989). To achieve these functions, some wood properties such as density change between (Muller-Landau 2004) and within tree species (Martínez-Vilalta et al. 2009; Fajardo 2016), and this variability could reflect balances between wood functions. Trade-offs determining wood density result from the conflict between filling the xylem with carbon-rich walls and parenchyma vs. leaving open conduit spaces (Carlquist 1975). A higher wood density provides greater strength but also entails higher construction costs (Niklas 1992). Globally, tree species forming narrow conduits and having high wood density show low growth rates (Chave et al. 2009). Conversely, conduit diameter increases in tree species with softer wood (Hacke and Sperry 2001; Bouche et al. 2014), thus providing a high hydraulic conductivity. Nevertheless, presumed conflicts in wood functions may reflect evolutionary paths of co-varying traits, and caution must be taken to interpret such assumed trade-offs (Larjavaara and Muller-Landau, 2010). In addition, wood density is a very conservative trait showing low variation along climatic gradients (Zhang et al. 2011). Nevertheless, since both radial growth and density determine forest carbon uptake, assessments of their responses to climate are required (Bouriaud et al. 2015).

Therefore, we need a better characterization of climate-growth-wood density associations. Conifers subjected to cold and drought stress, i.e. showing an overwhelming role of temperature and precipitation limitations on seasonal wood formation, offer a suitable system to perform such assessments because wood functions are mostly carried out by tracheids which are formed during a short growing season (Larson 1994). Here we address this question by considering three conifers of two genera from the Pinaceae family (*Pinus*, *Larix*). In conifers, wood density is related to

the ratio of cell-wall thickness to transversal lumen diameter (Yasue et al. 2000). This thickness–span ratio is considered a surrogate of xylem hydraulic functions since a large tracheid lumen (low thickness–span ratio) provides more hydraulic conductivity but increases the risk of frost- or drought-induced embolism (Hacke et al. 2001, 2015). Consequently, conifers should produce narrow earlywood tracheid lumens, which account for most hydraulic conductivity within the annual tree ring (Domec et al. 2009), and therefore a dense earlywood in response to dry conditions during the early growing season. However, large tracheid lumens have also been reported in Scots pine (*Pinus sylvestris*) provenances from dry sites (Martín et al. 2010) or in trees subjected to imposed dry conditions (Eilmann et al. 2011), and these patterns have been interpreted as responses to increase hydraulic conductivity. Therefore, more research is needed to ascertain how density responds to long-term changes in water availability during the growing season.

A negative association between minimum wood density and early growing-season (spring in the northern Hemisphere) precipitation was already observed in the Cupressaceae Spanish juniper (*Juniperus thurifera* L.) by studying forests subjected to cool-dry conditions (Camarero *et al*. 2014). Nevertheless, this relationship has to be investigated in Pinaceae species (e.g., pines, larches) which are widely distributed in cool-dry regions and form the world's largest conifer forest (Richardson 1998). A reduction in hydraulic conductivity would be linked to narrower tracheid lumens and higher minimum density values (Pittermann et al. 2006). Thus, we hypothesize that dry spring conditions would increase minimum wood density. Specifically, we aim: (i) to analyze how seasonal growth (earlywood and latewood widths) and density components respond to climate (mean monthly and seasonal temperature and total precipitation); and (ii) to test if minimum wood density is negatively associated to spring precipitation.

Materials and methods

Study sites and species

We selected four Eurasian regions from three countries subjected to cold and dry climatic conditions: Siberia and southern Urals in Russia, Khangai in Mongolia and Sierra de Gúdar in eastern Spain (Table 1). Continental climate conditions and low precipitation values explain why tree growth is constrained by drought during the growing season and a short growing season defined by long and cold winters in all the study areas (Block et al. 2004, Dulamsuren et al. 2009, Velisevich and Kozlov 2006, Devi et al. 2008, Knorre et al. 2010, Camarero et al. 2015). In Siberia and Mongolia we sampled larch (*Larix sibirica* Ledeb.) (see Supporting Information, Fig. S1), whilst Scots pine (*Pinus sylvestris* L.) was sampled in the Urals and Spain. In Spain we also sampled Black pine (*Pinus nigra* Arn. subsp. *salzmannii* (Dunal) Franco), a typical Mediterranean tree species (Richardson 1998). Note that the two most distant sites (Khangai in Mongolia and Sierra de Gúdar in Spain) are separated by ca. 7850 km.

The northernmost study region is located in Siberian forest-steppe zone where open larch forests are typical (Dylis 1961; Knorre et al., 2010). The forest sampled in the Urals is situated in the Aldan plateau where open conifer forests predominate up to 1250 m (Devi et al. 2008). In Mongolian lowlands, sampled trees formed forest-steppe ecotones which constitute the lower treeline (Treter 2000, Dulamsuren et al. 2010). The southernmost study region is located in the Sierra de Gúdar (southern Iberian Range, eastern Spain) and includes two Scots pine stands and two Black pine stands. In this area, the study sites were distributed along an elevational gradient because Scots pine dominates at cold Mediterranean sites situated at higher elevation, whereas Black pine is dominant at mid-elevation sites experiencing sub-Mediterranean transitional climates

(Camarero et al. 2015). We sampled one site (LR in Table 1) where the two species co-occurred to check for differences between species coexisting under similar climate and soil conditions. The selected study stands were not impacted by local anthropogenic disturbances (grazing, fires and logging) since the 1960s. The understory is dominated by shrubs in most study sites (e.g., *Juniperus communis* L.). Soils are brown in the Russian and Mongolian sites, where basic and clayey soils appear in Spain.

Field sampling

We randomly selected and sampled 15-30 dominant trees per site (on average 19 trees were sampled per site) with a minimum diameter of 20 cm at 1.3 m in ca. 1-ha large sampling areas. We also measured diameter at 1.3 m and total height of each tree using tapes and clinometers, respectively. Trees selected for sampling were dominant and had diameters ranging between 39.0 and 47.0 cm, heights between 9.3 and 10.5 m and ages (estimated at 1.3 m) between 79 and 318 years (Table 1). Stands are relatively open with basal area values ranging between 12 and 38 m^2 ha^{-1}.

We took two 5-mm wide cores at 1.3 m using Pressler increment borers, one of which was used for for densitometry analyses. We took special care for sampling this core perpendicular to the main stem so as to capture the main fibre direction. The one core was glued onto wooden mounts, sanded, visually cross-dated and checked for dating accuracy using dendrochronology (Fritts 2001).

Density measurements

One radial X-ray density profile was obtained from each tree using indirect X-ray densitometry. Prior to further treatment, resin was extracted from the wood samples with alcohol in a Soxhlet apparatus. Then, each core was cut carefully using a double-

bladed saw to obtain ca. 1.5-mm thick laths. These samples were air dried to moisture equilibrium and then subjected to X-ray exposure. The resulting X-ray films were scanned with microdensitometer DENDRO-2003 (Walesch Electroncs Ltd., Switzerland) with a resolution of 10 μm.. All densitometric analyses were performed at the Sukachev Institute of Forest (Krasnoyarsk, Russia).

The measured grey levels of tree-ring samples on the X-ray film were transferred to density values by comparing to a standard of known physical and optical density also exposed on the same film. For each annual ring, the following variables were obtained from the tree-ring density profiles: earlywood (EW hereafter) and latewood widths (LW hereafter), and minimum (MN hereafter) and maximum wood density (MX hereafter). Note that MN and MX are tightly related to earlywood and latewood mean densities, so we only analysed the former two variables because they were easier to define and showed a stronger response to climate variables (cf. Camarero et al. 2014). To define the earlywood-latewood transition we used the 50% level between the MN and MX values of each ring following Polge (1978) and confirmed this separation with a visual checking of the ring (Mäkinen and Hynynen 2014).

Climate data

We used local climate data (monthly total precipitation and mean temperature) for all study sites taken from the nearest meteorological stations (Table 2), excepting in Mongolian sites where climatic stations are located far from the sites. There, we obtained precipitation from the 0.5º grids covering each site and corresponding to the Climatic Research Unit (CRU) climate dataset (Harris et al. 2014). In Spain, local data from ten stations situated in the study area were converted into a regional climate series and elevation differences were corrected by calculating regressions between the station

elevation and mean annual temperature or total annual precipitation. To take into account the elevation difference among sampling sites, we corrected the regional mean temperature and precipitation data considering a mean lapse rate of -7.8 ºC km^{-1} and +420 mm km^{-1}, respectively (see more details in Sangüesa-Barreda et al. 2014). Climate data were obtained for the common period 1950-2002 when tree-ring data were available for all sites (Table 1).

To estimate the water balance at each study site, we estimated the potential evapotranspiration (PET) following the Hargreaves-Samani method (Hargreaves and Samani, 1982). Then, we calculated the annual water balance as the sum of the monthly differences between precipitation and PET. Lastly, we also calculated the Conrad continentality index to characterize the temperature range at each site (Tuhkanen, 1980).

Chronology building

We used the library dplR in the R platform to build the tree-ring (EW, LW, MN and MX) chronologies (Bunn, 2008). Prior to growth trend removal, power transformation was applied to density series. The individual tree-ring series were detrended to remove non-climatic age-related trends (Cook and Kairiukstis 1990). A 2/3 cubic smoothing spline with 50% frequency-response cut-off was fitted to the individual records and indexed values were calculated. Then, to remove part of the first-order autocorrelation, each indexed tree-ring series was subjected to autoregressive modelling so as to obtain residual indices. The residual indices were averaged on a year-by-year basis using a bi-weight robust mean, which reduced the effects of outliers, producing a site chronology for each species and variable.

To compare the chronologies, several statistics were calculated for the common 1950-2002 period considering either the raw series (mean; SD, standard deviation; AC

first-order autocorrelation) or the residual series (r_{bt}, mean correlation between trees; MSx, mean sensitivity, a measure of the relative variability between consecutive rings).

Statistical analyses

To compare tree-ring variables among species and sites, we performed one-way ANOVAs or and Kruskal-Wallis tests in the case data were normal or normality could not be assumed, respectively. These comparisons were followed by Tukey's Honest Significant Difference or Mann-Whitney *U* tests.

To evaluate how tree-ring variables were related, we calculated Pearson correlation coefficients between their residual series for each site and species considering the common 1950-2002 period. We also performed Principal Components Analysis (PCA) on variance-covariance matrices of residual width and density series to summarize their variability into a few principal components (Jolliffe 2002). Then, we calculated a second PCA based on the Pearson correlations obtained by relating the tree-ring variables with monthly climate data (mean temperature, precipitation) to summarize climate-growth and climate-density associations. Climate variables were considered from September prior to tree-ring formation up to October of the growth year based on previous studies on climate-growth relationships and xylogenesis (Kirdyanov et al. 2007, Camarero et al. 2010, 2015). The number of retained principal components in the first PCA was two because they explained at least 50% of the data variance (Jolliffe 2002). Analyses were done using the R package (R Development Core Team, 2015).

Results

Growth and density data

Some Scots pine (e.g., CA and PN sites) and larch (e.g., M0 and EF sites) sites presented higher EW and LW values than the other sites (Table 3). Conversely, Black pine stands presented the highest MN values, whereas larch stands showed the highest MX values. On average, MN showed the lowest mean AC values (0.35), whilst EW showed the highest AC average (0.64). The coherence between trees (r_{bt}) was significantly higher ($F = 2.53$, $P = 0.03$) in the case of seasonal width variables (EW, 0.49; LW, 0.51) than in the case of density variables (MN, 0.31; MX, 0.36). Note that the highest r_{bt} values for MN were observed for the Mediterranean Black pine sites. Lastly, the year-to-year variability (MSx) was low in the case of density variables (MN, 0.14; MX, 0.13), but significantly higher ($U = 0.99$, $P = 0.0001$) in the case of width variables (EW, 0.44; LW, 0.55).

Associations between tree-ring variables

Higher EW values were associated to higher LW values, particularly in the case of larch, but to lower MN values at all study sites (Table 4). More latewood production (higher LW values) was also related to heavy latewood (higher MX values) everywhere, but this association was again particularly strong for larch, which explains the positive EW-MX and the negative LW-MN associations observed at seven sites (i.e. all sites excepting the two Spanish high-elevation Scots pine forests). MN and MX were negatively associated, but this relationship was significant in two pine forests and the four larch sites.

Common patterns in width and density data between sites and species

According to the indexed series and the calculated PCAs, width and density data showed similarly consistent patterns between sites and species since the first principal

score (PC1) accounted for 35% of the variance (Figs. 1, 2 and 3). The second principal score (PC2) accounted for more variance in width than in density variables (21% vs. 15%; Fig. 3). The scores of EW and LW data of the same species, and also sites (e.g., LR site) grouped together in the PCA diagram with maximum scores on the PC1 and PC2 corresponding to LW data from the low-elevation and possibly dries Spanish sites and EW-LW data for the larch sites, respectively (Fig. 3a). Considering density data (Fig. 3b), MX and MN larch series showed the highest and lowest PC1 scores, in that order. The minimum PC2 scores were observed for MN data from the Black pine AC site.

Regarding the width series, low EW and LW values of the driest Black pine site (the low-elevation AC site) correspond to documented droughts (e.g., 1986 and 1994; Fig. 1). Low EW and LW values were also observed during the 1980s in Russia and Mongolia (Fig. 1). Regarding density data, low MX values were observed during cool summers in cold sites (e.g., 1972 in the high-elevation PN Scots pine site; 1976 in Russian and Mongolian sites; cf. Fig. 2). High MN density data were found during dry years (e.g., 1994 in Spain, 1979-1980 in Russia and Mongolia, 1986-1987 in Mongolia) and this pattern was most evident in dry sites as the Spanish AC site (Fig. 2).

Relationships between climate, width and density variables

The PC1s of PCAs based on climate-growth and climate-density matrices accounted for most common variance in the case of LW (50%) and MN (46%) data (see Supporting Information, Fig. S2). In both cases, Spanish sites grouped together and showed the highest PC1 scores, albeit the high-elevation PN Scots pine site showed a low PC1 score in the case of MN. In the PCAs based on EW and MX data, the PC1 separated the PN site from the rest of Spanish sites suggesting a different climate regime (i.e. cool-

wet vs. cool-dry downwards) at this high-elevation location. Larch sites also grouped together and showed high PC2 scores in the LW and MN PCAs.

The correlation analyses between width and density data and the resulting PC1 scores and climate variables showed that wet and cool spring (May to June) conditions enhanced EW formation but lead to low MN values, i.e. dry spring conditions were associated to low EW and high MN (Fig. 4; see also Supporting Information, Table S1). LW formation was enhanced by wet-cool conditions during the late growing season (July), particularly in Spanish (excluding the high-elevation PN site) and Mongolian larch sites. MX increased in response to high June-July precipitation values and low temperatures in the driest sites (LR and AC sites in Spain, M7 site in Mongolia).

In absolute terms, the strongest associations between climate and width or density variables were found for May or June precipitation and MN (Fig. 5; see also Supporting Information, Table S1). These negative precipitation-MN associations were observed for the three study species and countries. The strongest precipitation-MN associations were either observed in May (Spain, Black pine AC site; Russia, CA Scots pine CA site) or June (e.g., Mongolian M7 larch site) (Fig. 5). May or June precipitation explained ca. 32-42% of the MN variance in these drought-prone sites.

Discussion

As we hypothesized, dry spring conditions were associated to high MN values and consequently a dense earlywood (Fig. 5). This finding agrees with our expectations that water deficit during the early growing season, when the earlywood is formed and minimum wood density along the annual tree ring is observed (Vaganov et al. 2009). Such water shortage would lead to the formation of a dense earlywood characterized by

tracheids with narrow lumens and a decreased hydraulic conductivity (Domec et al. 2009).

Our findings are consistent with the negative association between minimum wood density and spring precipitation reported for semi-arid sites (Cleaveland, 1986). Improved water status has been linked to a lower density in Norway spruce (*Picea abies*) (Lundgren, 2004). Such precipitation-density coupling, possibly mediated by a conductivity reduction, could also explain the decrease in earlywood production observed in response to water deficit in drought-prone sites from the forest-steppe and Mediterranean biomes (e.g., Dulamsuren et al. 2010; Camarero et al. 2015). According to ecophysiological studies, in these cool-dry regions photosynthesis rates decrease in winter and summer and growing-season drought stress, caused by elevated atmospheric vapour pressure deficit and low soil water availability, leads to radial-growth reduction (Dulamsuren et al. 2009; Gimeno et al. 2012). Nevertheless, the correlations between spring precipitation and MN were always stronger, in absolute terms, than those detected between rainfall EW (Figs. 4 and 5; Table S1). Consequently, MN plays a distinct response to climate, and it is a robust climate proxy.

The correlations found between MN and spring precipitation in pine and larch (Fig. 5) were similar to those observed in Spanish juniper (Camarero et al. 2014), explaining on average 37% of MN variability, which indicates further investigations should be made on climate-MN associations. This research could explicitly consider wood anatomy to disentangle if MN changes are mainly due to lumen modifications, as we assume, or to changes in cell-wall thickness. For instance, in drought-exposed Norway spruce trees, the ring wood density augmented as a consequence of the formation of thicker cell walls (Jyske et al. 2010), whilst the increased tracheid lignin content was observed in drought-stressed Austrian pines (*Pinus nigra*) (Gindl 2001).

The climate-MN associations could also reflect adaptive responses to drought stress. For instance, Douglas fir (*Pseudotsuga menziesii*) trees showing high resistance to xylem cavitation and lower drought-induced mortality also presented the highest minimum wood density values (Dalla-Salda et al. 2009; Ruiz Diaz Britez et al. 2014), which could reflect more narrow tracheid lumens. Nevertheless, other parameters affecting cavitation and hydraulic conductivity should be also considered including conduit length, pit size and the numbers of tracheids per unit area (Carlquist 1975).

Width and density variables of tree-rings provide redundant information (Kirdyanov et al. 2007, Büntgen et al. 2010, Vaganov and Kirdyanov 2010, Galván et al. 2015). This limitation could apply to MN which is negatively related to EW and both variables show opposite associations with rainfall (Tables 4 and S1). Note that we opted for analysing indexed growth and density values without removing dependences between them (e.g., EW-MN and LW-MX relationships) since our purpose was to assess how climate influenced seasonal growth and density data. Conversely, a pro of analysing MN is that it offers indirect clues on wood phenology. For example, the shift in the strongest precipitation-MN association from May (Spanish and Russian sites) to June (Mongolian sites; Fig. 5) could be caused by a late peak of earlywood formation in Mongolian sites. This agrees with our knowledge of xylogenesis with maximum rates of tracheid production in Spanish pines occurring in May (Camarero et al. 2010).

In the northern Siberian larch forests, width and density variables mainly respond to temperature changes during the short growing-season (June to July) (Esper et al. 2010) and indirectly to winter precipitation which affects the snow melting and soil temperatures (Vaganov et al. 1999, Kirdyanov et al. 2003). But we have also evidenced that in sites subjected to water shortage spring precipitation in the south of Siberia is also negatively related to MN (Figs. 4 and 5) suggesting that earlywood tracheid

expansion is constrained by water availability. A low soil temperature can reduce water viscosity leading to a high root hydraulic resistance and decreasing the flow of water from the soil to the tree and reducing the stomatal conductance (Wan et al. 2001). Spring cold conditions could therefore affect soil water viscosity constraining the radial enlargement of earlywood tracheids.

In cool-arid Inner Asian forests, wet conditions during the growing season enhance radial growth (Poulter et al. 2013). In fact, Mongolian forest-steppe ecotones are experiencing warmer and drier conditions since the 1940s, causing growth decline and the retreat of larch forests (Dulamsuren et al. 2010). Increased aridity and drought stress are major restrictions of tree growth and functioning in these biomes where larches show low shoot water potentials and high stomatal conductance (Dulamsuren et al. 2009). These constrains agree with our findings and emphasize the key role played by sufficient moisture availability for growth and wood formation.

In Mediterranean pine forests, wet conditions during the previous winter and the current spring are associated to improved earlywood production (De Luis et al. 2007, Martín-Benito et al. 2008, Pasho et al. 2012) and a decrease in MN (Olivar et al. 2015). Wet conditions favouring tracheid division and radial enlargement should result in low MN (Bouriaud et al. 2005), as we found mainly in the low-elevation driest sites (Fig. 5). Under more continental and colder conditions, cambial resumption is delayed and summer precipitation and temperature become more relevant as drivers of growth in species as Scots pine (Sánchez-Salguero et al. 2015). This explains why earlywood density may not be related to spring precipitation in some Mediterranean Scots pine stands (Olivar et al. 2015). In contrast, high-elevation Scots pine stands (e.g., the PN site) presented a positive association between summer temperatures and maximum density (Table S1) which is well established in cold biomes as boreal and subalpine

forests (e.g., Briffa et al. 1998). This relationship was also previously reported (Olivar et al. 2015), and it is due to an improved thickening and lignification of latewood cell-walls in response to warmer conditions (Gindl et al. 2000; Yasue et al. 2000).

An increasing influence of climate warming on temporal coherence in ring-width records (spatial synchrony) have been observed across some of the studied Eurasian regions (Shestakova et al. 2016). It could be tested if this enhanced synchrony holds too for density records at similar sub-continental scales since wood density seasonal components (MN, MX) respond to different climate variables, and wood density is a fundamental variable to estimate forest carbon uptake and woody biomass pools (Bouriaud et al. 2015). It is expected that growing-season precipitation patterns would drive earlywood density and hydraulic conductivity (Pacheco et al. 2016). Consequently, we predict that warmer and drier conditions during the most active phase of the growing season would reduce earlywood production but rise earlywood density.

To conclude, minimum wood density of three conifer species (*L. sibirica*, *P. sylvestris* and *P. nigra*) reflects changes in growing-season (spring) precipitation in cool-dry Eurasian regions. An increase in minimum wood density in response to dry spring conditions was observed in drought-prone sites from the forest-steppe and Mediterranean biomes. The associations between minimum wood density and precipitation were stronger than those observed with seasonal width variables. Forecasted drier conditions during the growing season would increase minimum wood density and reduce radial growth negatively affecting the ability of the studied Eurasian forests to fix and store carbon pools as stem wood.

Acknowledgements

We acknowledge the support of Spanish Ministry of Economy project (Fundiver, CGL2015-69186-C2-1-R). Tree-ring density data were obtained and preliminary analyzes under support of Russian Science Foundation (project 14-14-00295). Jordi?

References

Block J, Magda VN, Vaganov EA. 2004. Temporal and spatial variability of tree growth in mountain forest steppe in Central Asia. In: Jansma E, Bräuning A, Gärtner H, Schleser G (eds.) (2004) TRACE - Tree Rings in Archaeology, Climatology and Ecology 44: 46–53.

Bouche, P.S., Larter, M., Domec, J.C., Burlett, R., Gasson, P., Jansen, S. and Delzon, S., 2014. A broad survey of hydraulic and mechanical safety in the xylem of conifers. Journal of Experimental Botany 65: 4419–4431.

Bouriaud, O., Leban, J., Bert, D., Deleuze, C. 2005. Intra-annual variations in climate influence growth and wood density of Norway spruce Intra-annual variations in climate influence growth and wood density. Tree Physiology 25: 651–660.

Bouriaud, O., Teodosiu, M., Kirdyanov, A.V. and Wirth, C. 2015. Influence of wood density in tree-ring-based annual productivity assessments and its errors in Norway spruce. Biogeosciences 12: 6205–6217.

Briffa, K.R., Schweingruber, F.H., Jones, P.D., Osborn, T.J., Shiyatov, S.G., and Vaganov, E.A. 1998. Reduced sensitivity of recent tree-growth to temperature at high northern latitudes. Nature 391: 678–682.

Bunn, A.G. 2008. A dendrochronology program library in R (dplR). Dendrochronologia 26: 115–124.

Büntgen, U., Frank, D., Trouet, V. And Esper, J. 2010. Diverse climate sensitivity of Mediterranean tree-ring width and density. Trees, Struct. and Funct. 24: 261–273.

Camarero, J.J., Olano, J.M. and Parras, A. 2010. Plastic bimodal xylogenesis in conifers from continental Mediterranean climates. New Phytologist 185: 471-480.

Camarero, J.J., Rozas, V. and Olano, J.M. 2014. Minimum wood density of *Juniperus thurifera* is a robust proxy of spring water availability in a continental Mediterranean climate. Journal of Biogeography 41: 1105–1114.

Camarero, J.J., Gazol, A., Tardif, J.C. and Conciatori, F. 2015. Attributing forest responses to global-change drivers: limited evidence of a CO_2-fertilization effect in Iberian pine growth. Journal of Biogeography 42: 2220–2233.

Camarero, J.J., Guada, G., Sánchez-Salguero, R. and Cervantes, E. 2016. Winter drought impairs xylem phenology, anatomy and growth in Mediterranean Scots pine forests. Tree Physiology 36: 1536-1549.

Carlquist, S. 1975. Ecological Strategies of Xylem Evolution. University of California Press, Berkeley, USA.

Chave, J., Coomes, D., Jansen, S., Lewis, S.L., Swenson, N.G. & Zanne, A.E. 2009. Towards a worldwide wood economics spectrum. Ecology Letters 12: 351–366.

Cleaveland, M.K. 1986. Climatic response of densitometric properties in semiarid site tree rings. Tree-Ring Bulletin 46: 13–29.

Cook, E.R., Kairiukstis, L.A., 1990. Methods of Dendrochronology: Applications in the Environmental Science. Kluwer Academic Publishers, Dordrecht.

Dalla-Sala, G., Martínez-Mier, A., Cochard, H., Rozenberg, P. 2009. Variation of wood density and hydraulic properties of Douglas-fir (*Pseudotsuga menziesii* (Mirb.) Franco) clones related to a heat and drought wave in France. Forest Ecology and Management 257: 182–189.

De Luis M, Gričar J, Čufar K, Raventós J, 2007. Seasonal dynamics of wood formation in *Pinus halepensis* from dry and semi-arid ecosystems in Spain. IAWA J. 28: 389-404.

Devi, N., Hagedorn, F., Moiseev, P., Bugmann, H., Shiyatov, S., Mazepa, V. and Rigling, A. 2008. Expanding forests and changing growth forms of Siberian larch at the Polar Urals treeline during the 20th century. Global Change Biology 14: 1581–1591.

Domec, J.C., Warren, J.M., Meinzer, F.C., Lachenbruch, B. 2009. Safety factors for xylem failure by implosion and air-seeding within roots, trunks and branches of young and old conifer trees. IAWA Journal 30: 101–120.

Dulamsuren, Ch., Hauck, M., Bader, M., Osokhjargal, D., Oyungerel, S., Nyambayar, S., Runge, M., Leuschner, C. 2009. Water relations and photosynthetic performance in *Larix sibirica* growing in the forest-steppe ecotone of northern Mongolia. Tree Physiology 29: 99–110.

Dulamsuren, Ch., Hauck, M., Leuschner, C. 2010. Recent drought stress leads to growth reductions in *Larix sibirica* in the western Khentey, Mongolia. Global Change Biology 16: 3024–3035.

Dylis, NV. 1961. Listvennitsa Vostochnoi Sibiri i Dal'nego Vostoka. Izmenchivost' i prirodnoe raznoobrazie (Larch in Eastern Siberia and the Far East: Variation and Natural Diversity). Akad. Nauk SSSR, Moscow.

Eilmann, B., Zweifel R., Buchmann, N., Pannatier, E.G. & Rigling, A. (2011) Drought alters timing, quantity, and quality of wood formation in Scots pine. Journal of Experimental Botany 62: 2763–2771.

Esper, J., Frank, D., Büntgen, U., Verstege, A., Hantemirov, R.M., Kirdyanov A.V. 2010. Trends and uncertainties in Siberian indicators of 20th century warming. Global Change Biology 16: 386-398.

Fajardo, A. 2016. Wood density is a poor predictor of competitive ability among individuals of the same species. Forest Ecology and Management 372: 217–225.

Fritts, H.C. 2001. Tree Rings and Climate. Blackburn Press, Caldwell, NJ.

Galván, D.J., Büntgen, U., Ginzler, C., Grudd, H., Gutiérrez, E., Labuhn, I. and Camarero, J.J. 2015. Drought-induced weakening of growth-temperature associations in high-elevation Iberian pines. Global and Planetary Change 124: 95-106.

Gimeno, T.E., Camarero, J.J., Granda, E., Pías, B. and Valladares, F. 2012. Enhanced growth of *Juniperus thurifera* under a warmer climate is explained by a positive carbon gain under cold and drought. Tree Physiology 32: 326–336.

Gindl, W. 2001. Cell-wall lignin content related to tracheid dimensions in drought-sensitive Austrian pine (*Pinus nigra*). IAWA J. 22: 113–120.

Gindl, W., Grabner, M. & Wimmer, R. 2000. The influence of temperature on latewood lignin content in treeline Norway spruce compared with maximum density and ring width. Trees, Struct. and Funct. 14: 409–414.

Hacke, U.G., & Sperry, J.S. 2001. Functional and ecological xylem anatomy. Perspectives in Plant Ecology, Evolution and Systematics 4: 97-115.

Hacke, U.G., Sperry, J.S., Pockman, W.T., Davis, S.D. & McCulloh, K.A. 2001. Trends in wood density and structure are linked to prevention of xylem implosion by negative pressure. Oecologia, 126, 457–461.

Hacke U.G., Lachenbruch B., Pittermann J., Mayr S., Domec J.-C., Schulte P.J. 2015. The hydraulic architecture of conifers. In: Functional and Ecological Xylem Anatomy (ed. U.G. Hacke). Springer, Berlin, Heidelberg, pp. 39-75.

Hargreaves, G.H., Samani, Z.A., 1982. Estimating potential evapotranspiration. J. Irrig. Drain. Eng. 108, 225–230.

Harris, I., Jones, P.D., Osborn, T.J. and Lister, D.H. 2014. Updated high-resolution grids of monthly climatic observations - the CRU TS3.10 Dataset. International Journal of Climatology 34: 623-642

Jolliffe, I. 2002. Principal Component Analysis. Springer, New York.

Jyske, T., Hölttä, T., Mäkinen, H., Nöjd, P., Lumme, I. & Spiecker, H. (2010) The effect of artificially induced drought on radial increment and wood properties of Norway spruce. Tree Physiology 30: 103–115.

Kirdyanov A.V., Hughes M.K., Vaganov E.A., Schweingruber F., Silkin P. 2003. The importance of early summer temperature and date of snow melt for tree growth in Siberian Subarctic. Trees, Struct and Funct. 17: 61–69.

Kirdyanov A.V., Vaganov E.A., Hughes, M.K. 2007. Separating the climatic signal from tree-ring width and maximum latewood density records. Trees, Struct. Funct 21: 37–44.

Knorre A.A., Siegwolf R.T.W., Saurer M., Sidorova O.V., Vaganov E.A., Kirdyanov A.V. 2010. Twentieth century trends in tree ring stable isotopes (δ13C and δ18O) of Larix sibirica under dry conditions in the forest steppe in Siberia. J. Geophys. Res.: Biogeosciences, v. 115, G03002.Larjavaara M, Muller-Landau HC. 2010. Rethinking the value of high wood density. Functional Ecology 24: 701–705.

Larson, P.R. 1994. The Vascular Cambium: Development and Structure. Springer, New York.

Lundgren, C. 2004. Microfibril angle and density patterns of fertilized and irrigated Norway spruce. Silva Fennica 38: 107–117.

Mäkinen H, Hynynen J. 2014. Wood density and tracheid properties of Scots pine: responses to repeated fertilization and timing of the first commercial thinning. Forestry 87: 437–447.

Martín, J.A., Esteban, L.G., de Palacios, P. & Fernández, F.G. (2010) Variation in wood anatomical traits of *Pinus sylvestris* L. between Spanish regions of provenance. Trees, Struct and Funct. 24: 1017–1028.

Martín-Benito D, Cherubini P, Del Río M, Cañellas I (2008) Growth response to climate and drought in *Pinus nigra* Arn. trees of different crown classes. Trees 22: 363-373.

Martínez-Vilalta J, Cochard H, Mencuccini M, Sterck F, Herrero A, Korhonen J, Llorens P, Nikinmaa E, Nolè A, Poyatos R (2009) Hydraulic adjustment of Scots pine across Europe. New Phytol 184: 353–364.

Muller-Landau, H.C. (2004) Interspecific and inter-site variation in wood specific gravity of tropical trees. Biotropica 36: 20–32.

Niklas, K.J. 1992. Plant Biomechanics. University of Chicago Press, Chicago.

Olivar J, Rathgeber C, Bravo F. 2015. Climate change, tree-ring width and wood density of pines in Mediterranean environments. IAWA Journal 36: 257-269.

Pacheco, A., Camarero, J.J. and Carrer, M. 2016. Linking wood anatomy and xylogenesis allows pinpointing of climate and drought influences on growth of coexisting conifers in continental Mediterranean climate. Tree Physiology 36: 502–512

Pasho, E., Camarero, J.J. and Vicente-Serrano, S.M. 2012. Climatic impacts and drought control of radial growth and seasonal wood formation in *Pinus halepensis*. Trees: Structure and Function 26: 1875–1886.

Pittermann J., Sperry, J.S., Wheeler, J.K., Hacke, U.G. and Sikkema, E.H. 2006. Mechanical reinforcement of tracheids compromises the hydraulic efficiency of conifer xylem. Plant, Cell and Environment 29: 1618–1628.

Polge, H. 1978. Fifteen years of wood radiation densitometry. Wood Sci. Technol. 12: 187–196.

Poulter, B. Pederson, N., Liu, H., Zhu Z., D'Arrigo, R., Ciais, P., Davi, N., Frank, D., Leland, C., Myneni, R., Piao, S. and Wang, T. 2013. Recent trends in Inner Asian forest dynamics to temperature and precipitation indicate high sensitivity to climate change. Agric. For. Meteorol. 178–179: 31–45.

R Development Core Team. 2015. R: A Language and Environment for Statistical Computing. In. *R Foundation for Statistical Computing*, Vienna, Austria.

Richardson D.M. 1998. Ecology and Biogeography of Pinus. Cambridge Univ Press, Cambridge, UK.

Ruiz Diaz Britez M, Sergent A-S, Martinez Meier A, Bréda N, Rozenberg P (2014) Wood density proxies of adaptive traits linked with resistance to drought in Douglas fir (*Pseudotsuga menziesii* (Mirb.) Franco). Trees 28:1289–1304

Sánchez-Salguero, R., Camarero, J.J., Hevia, A., Madrigal-González, J., Linares, J.C., Ballesteros-Canovas, J.A., Sánchez-Miranda, A., Alfaro-Sánchez, R., Sangüesa-Barreda, S., Galván, J.D., Gutiérrez, E., Génova, M. and Rigling, A. 2015. What drives growth of Scots pine in continental Mediterranean climates: Drought, low temperatures or both? Agricultural and Forest Meteorology 206: 151-162.

Sangüesa-Barreda, G., Camarero, J.J., García-Martín, A., Hernández, R. & de la Riva, J. (2014) Remote-sensing and tree-ring based characterization of forest defoliation and growth loss due to the Mediterranean pine processionary moth. Forest Ecology and Management, 320, 171–181.

Shestakova, T.A., Gutiérrez, E., Kirdyanov, A.V., Camarero, J.J., Génova, M., Knorre, A.A., Linares, J.C., Resco de Dios, V., Sánchez-Salguero, R. and Voltas, J. 2016.

Forests synchronize their growth in contrasting Eurasian regions in response to climate warming. PNAS 113: 662-667.

Treter U. 2000. Stand structure and growth patterns of the larch forests of Western Mongolia –a dendrochronological approach. Geowiss. Abh. Reihe A 205:60-66.

Tuhkanen, S. 1980. Climatic parameters and indices in plant geography. Acta Phytogeogr Suecica 67: 1–110.

Vaganov E.A., Hughes M.K., Kirdyanov A.V., Schweingruber F.H., Silkin P.P. 1999. Influence of snowfall and melt timing on tree growth in subarctic Eurasia. Nature 400: 149–151.

Vaganov, E.A., Schulze, E.-D., Skomarkova, M.V., Knohl, A., Brand, W.A. & Roscher, C. 2009. Intra-annual variability of anatomical structure and $\delta^{13}C$ values within tree rings of spruce and pine in alpine, temperate and boreal Europe. Oecologia, 161: 729–745.

Vaganov E.A., Kirdyanov A.V. 2010. Dendrochronology of larch trees growing on Siberian permafrost. In: A. Osawa, O.A. Zyryanova, Y. Matsuura, T. Kajimoto and R. W. Wein (eds.), Permafrost Ecosystems: Siberian Larch Forests, Ecological studies, Vol. 209, Springer, Heidelberg, pp. 347-363.

Velisevich SN, Kozlov DS (2006) Effects of temperature and precipitation on radial growth of Siberian Larch in ecotopes with optimal, insufficient, and excessive soil moistening. Russian Journal of Ecology 37: 241–246.

Wan X, Zwiazek JJ, Lieffers VJ, Landhäusser SM (2001) Hydraulic conductance in aspen (*Populus tremuloides*) seedlings exposed to low root temperatures. Tree Physiol 21:691–696.

Yasue, K., Funada, R., Kobayashi, O., Ohtani, J. (2000) The effects of tracheid dimensions on variations in maximum density of *Picea glehnii* and relationships to climatic factors. Trees, Struct and Funct. 14: 223–229.

Zhang, S.-B., Ferry Silk, J.W., Zhang, J.-L., Cao, K.-F. 2011. Spatial patterns of wood traits in China are controlled by phylogeny and the environment. Glob. Ecol. Biogeogr. 20: 241–250.

Zobel B.J., van Buijtenen J.P. 1989. Wood variation. Its causes and control. Springer-Verlag, Berlin.

Tables

Table 1. Characteristics of the study sites. Age values are means ± SD.

Region (country)	Species (code)	Site (code)	Latitude(N)	Longitude	Elevation (m a.s.l.)	No. trees	Age at 1.3 m (years)	Timespan with > 5 trees
Siberia (Russia)	*Larix sibirica* (Ls)	Efremkino (EF)	54º 29’	89º 28’ E	520	17	194 ± 49	1766-2002
		Shira (KH)	54º 24’	89º 58’ E	590	24	142 ± 40	1877-2005
Southern Urals (Russia)	*Pinus sylvestris* (Ps)	Aldanskoye (CA)	52º 11’	59º 44’ E	740	16	80 ± 9	1902-2005
Khangai (Mongolia)	*Larix sibirica* (Ls)	Khangai 2 (M7)	47º 24’	100º 43’ E	1920	24	137 ± 75	1838-2002
		Khangai 1 (M0)	46º 44’	102º 40’ E	1870	30	228 ± 80	1695-2002
Sierra de Gúdar (Spain)	*Pinus sylvestris* (Ps)	Peñarroya (PN)	42º 23’	0º 39’ W	2020	16	79 ± 19	1906-2011
		Las Roquetas (LR)	40º 19’	0º 43’ W	1615	15	103 ± 20	1875-2011
	Pinus nigra (Pn)	Las Roquetas (LR)	40º 19’	0º 43’ W	1615	15	131 ± 33	1847-2011
		Alto de Cabra (AC)	40º 20’	0º 48’ W	1090	16	120 ± 21	1859-2011

Table 2. Climatic characterization of the study sites calculated for the common period 1950-2002. Sites' and species' codes are as in Table 1.

Region (country)	Study sites (species)	Closest meteorological station (coordinates)	Mean annual temperature (ºC)	Annual precipitation (mm)	Annual water balance (mm)	Continentality index (type)
Siberia (Russia)	EF (Ls), KH (Ls)	Shira (54º 29' N, 89º 58' E, 448 m a.s.l.)	-1.9 º	316	-161	63 (Continental)
S. Urals (Russia)	CA (Ps)	Bredy (52º 25' N, 60º 20' E, 305 m a.s.l.)	2.4 º	352	-240	60 (Continental)
Khangai (Mongolia)	M7 (Ls), M0 (Ls)	Tsetserleg (47º 24' N, 101º 01' E, 1691 m a.s.l.)	0.4 º	331	-124	50 (Sub-continental)
Gúdar (Spain)	PN (Ps), LR (Ps), LR (Pn), AC (Pn)	Mora de Rubielos (40º 15' N, 0º 45' W, 1038 m a.s.l.)	9.5	533	-849	26 (Oceanic)

Table 3. Comparison of the dendrochronological statistics calculated for the standard (mean, SD, AC) and residual chronologies (r_{bt} and MSx) of the three tree species considering three variables (EW, earlywood width; LW, latewood width; MN, minimum wood density; MX, maximum wood density). Values were calculated for the common 1950-2002 period. Statistics abbreviations: AC, first-order autocorrelation; r_{bt}, mean correlation between trees; MSx, mean sensitivity. Significant ($P < 0.05$) differences between species are indicated by different letters according to Tukey's Honest Significant Difference (r_{bt}) or Mann-Whitney *U* tests (MSx).

Species	Site	EW				LW			
		Mean ± SD (mm)	**AC**	**r_{bt}**	**MSx**	**Mean ± SD (mm)**	**AC**	**r_{bt}**	**MSx**
Pinus sylvestris	CA	0.97 ± 0.17 b	0.52	0.41	0.39	0.22 ± 0.08 ab	0.32	0.49	0.62
	LR	0.80 ± 0.16 ab	0.65	0.46	0.35	0.20 ± 0.06 ab	0.41	0.54	0.58
	PN	1.05 ± 0.18 b	0.58	0.62	0.48	0.26 ± 0.08 b	0.60	0.46	0.46
Pinus nigra	AC	0.47 ± 0.07 a	0.62	0.55	0.52	0.15 ± 0.04 a	0.50	0.48	0.55
	LR	0.56 ± 0.13 a	0.69	0.48	0.38	0.18 ± 0.06 a	0.39	0.55	0.60
Larix sibirica	EF	0.58 ± 0.15 a	0.71	0.63	0.54	0.24 ± 0.09 ab	0.63	0.52	0.59
	KH	0.36 ± 0.17 a	0.54	0.66	0.63	0.10 ± 0.02 a	0.51	0.51	0.60
	M7	0.37 ± 0.06 a	0.78	0.33	0.26	0.13 ± 0.03 a	0.41	0.48	0.54
	M0	0.78 ± 0.15 ab	0.68	0.45	0.38	0.21 ± 0.05 ab	0.61	0.36	0.42
		MN				**MX**			
		Mean ± SD (g cm^{-3})	**AC**	**r_{bt}**	**MSx**	**Mean ± SD (g cm^{-3})**	**AC**	**r_{bt}**	**MSx**
Pinus sylvestris	CA	0.28 ± 0.01 a	0.39	0.31	0.27	0.82 ± 0.03 a	0.41	0.26	0.14
	LR	0.33 ± 0.02 ab	0.30	0.34	0.11	0.89 ± 0.05 ab	0.36	0.35	0.11
	PN	0.30 ± 0.02 ab	0.41	0.25	0.09	0.82 ± 0.03 a	0.39	0.32	0.12
Pinus nigra	AC	0.39 ± 0.02 b	0.22	0.40	0.16	0.88 ± 0.04 ab	0.32	0.39	0.13
	LR	0.35 ± 0.01 ab	0.35	0.38	0.11	0.85 ± 0.04 a	0.43	0.38	0.10
Larix sibirica	EF	0.28 ± 0.02 a	0.37	0.31	0.15	0.93 ± 0.04 b	0.40	0.37	0.17
	KH	0.32 ± 0.02 ab	0.34	0.32	0.15	0.90 ± 0.03 ab	0.34	0.43	0.18
	M7	0.27 ± 0.01 a	0.46	0.25	0.10	0.93 ± 0.05 b	0.51	0.34	0.10
	M0	0.28 ± 0.01 a	0.35	0.26	0.14	0.94 ± 0.06 b	0.41	0.37	0.13

Table 4. Correlations (Pearson coefficients) calculated between the residual chronologies of tree-ring variables (EW, earlywood width; LW, latewood width; MN, minimum wood density; MX, maximum wood density). Correlations were calculated for the common 1950-2002 period and values with $P > 0.05$ are underlined. The last row shows the number of significant ($P < 0.05$) positive (+) and negative (−) correlations.

Species	Site	EW-LW	EW-MN	EW-MX	LW-MN	LW-MX	MN-MX
Pinus sylvestris	CA	0.39	-0.41	0.55	-0.32	0.43	-0.36
	LR	0.34	-0.71	0.22	-0.23	0.55	-0.14
	PN	0.28	-0.38	0.02	-0.19	0.28	-0.04
Pinus nigra	AC	0.60	-0.81	0.65	-0.34	0.64	-0.49
	LR	0.45	-0.73	0.44	-0.34	0.53	-0.19
Larix sibirica	EF	0.70	-0.75	0.81	-0.45	0.72	-0.73
	KH	0.75	-0.70	0.76	-0.41	0.80	-0.45
	M7	0.81	-0.69	0.31	-0.45	0.68	-0.34
	M0	0.87	-0.66	0.80	-0.52	0.74	-0.68
Sign of the correlation		+ −	+ −	+ −	+ −	+ −	+ −
No. significant correlations		9 0	0 9	7 0	0 7	9 0	0 6

Figures

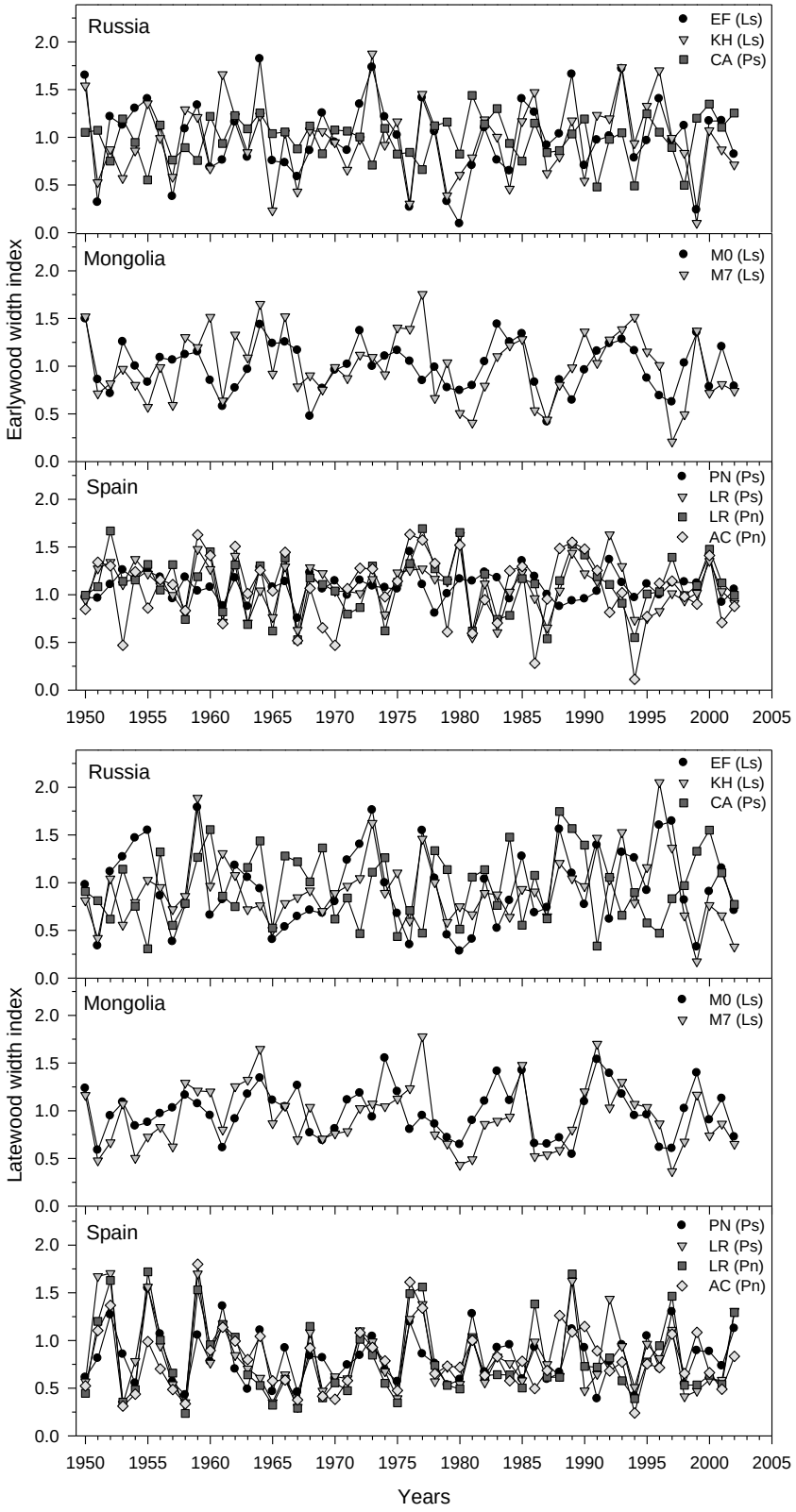

Figure 1. Earlywood and latewood series of indexed values for the nine study sites abbreviated as in Table 1. Graphs are plotted for each country. Tree species are abbreviated by the codes written between parentheses (Ps, *Pinus sylvestris*; Pn, *Pinus nigra*; Ls, *Larix sibirica*).

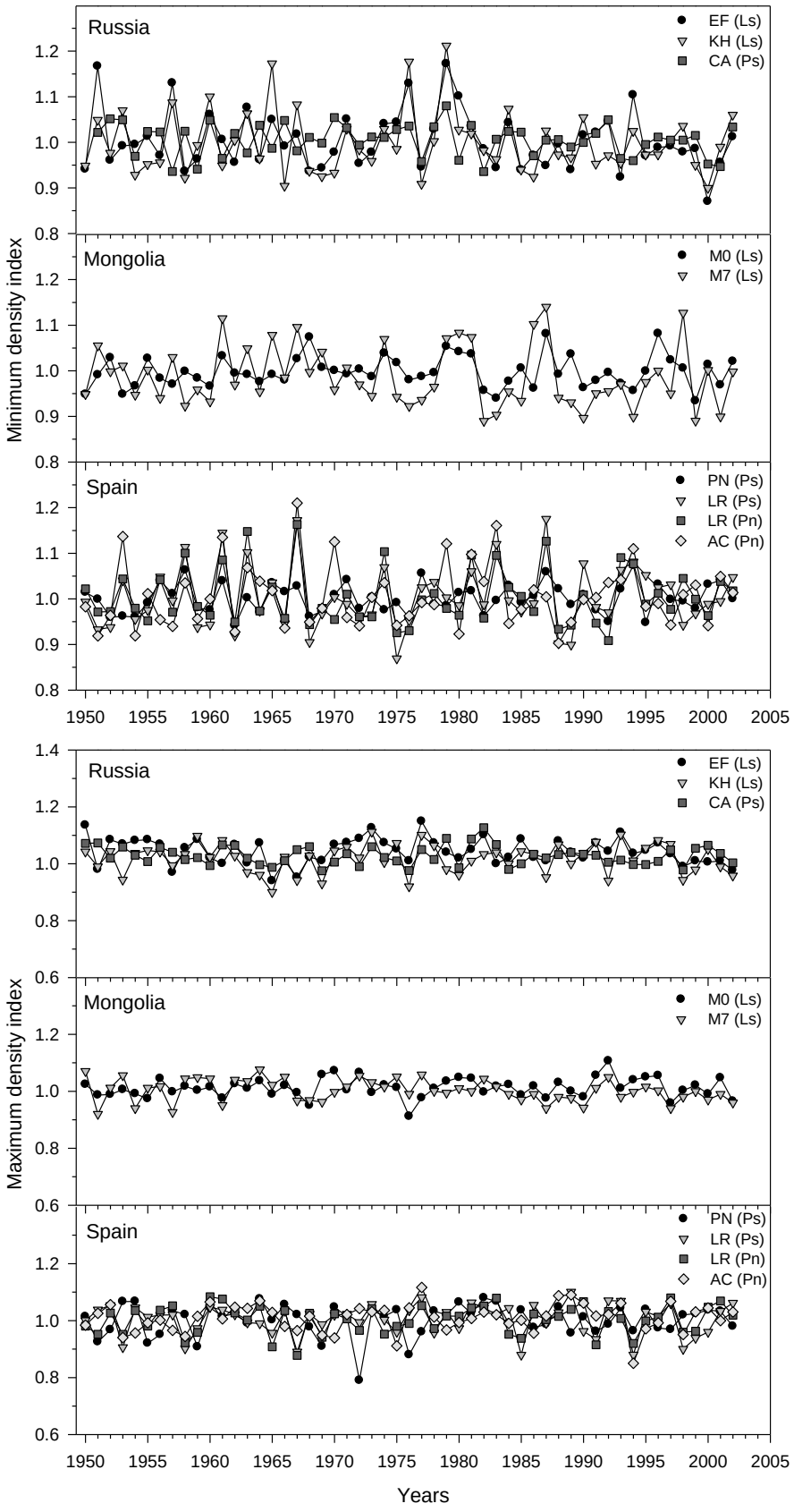

Figure 2. Minimum and maximum density series of indexed values for the nine study sites abbreviated as in Table 1. Rest of explanations are as in Figure 1.

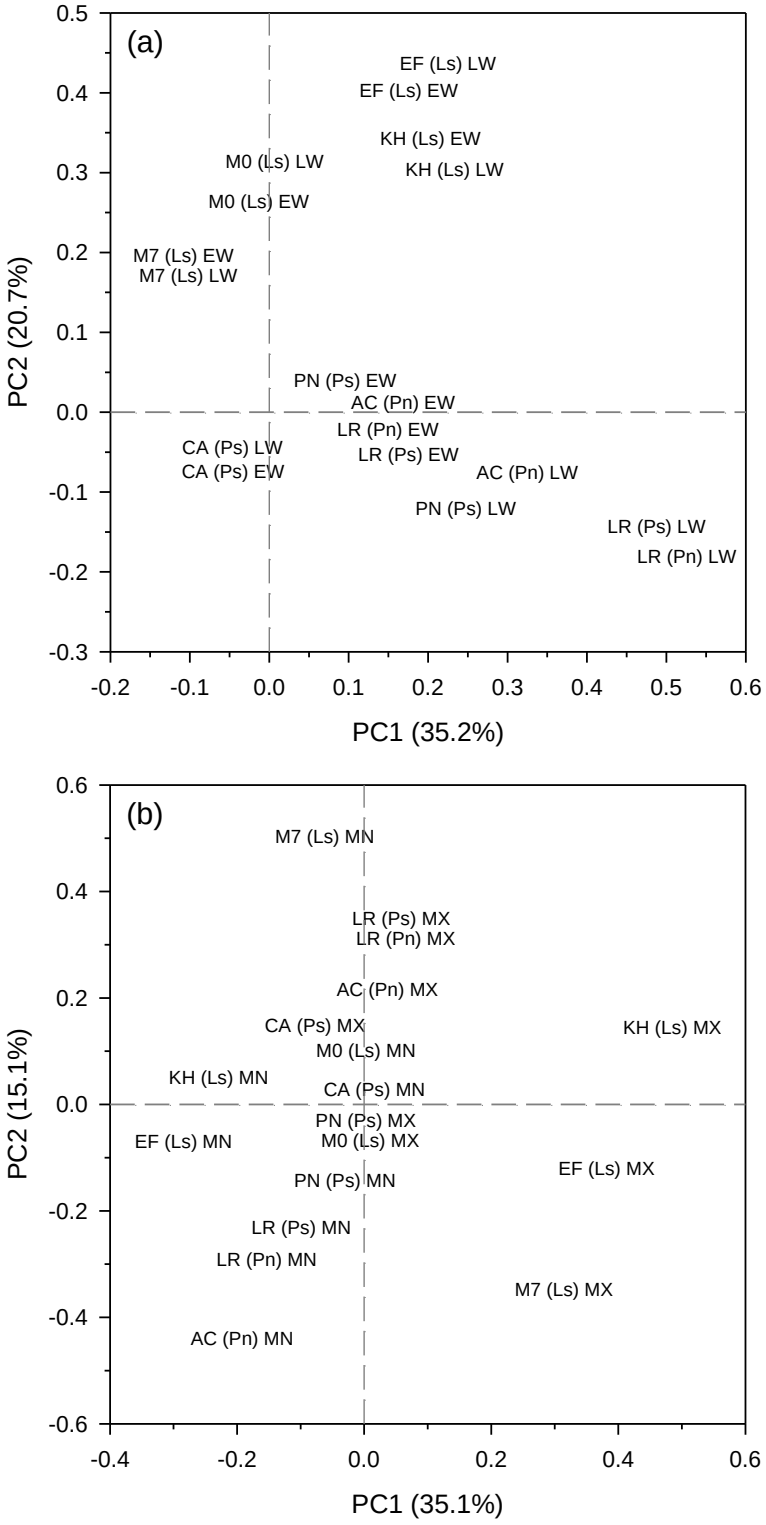

Figure 3. Scatters showing the scores of the first (PC1) and second (PC2) principal components obtained by calculating Principal Component Analyses on the variance-covariance matrices of residual width (a) and density (b) series. In the upper plot EW and LW indicate earlywood and latewood widths, respectively. In the lower plot MN and MX indicate minimum and maximum wood densities, respectively. Sites are abbreviated by two-letter codes as in Table 1. Tree species are abbreviated by the codes written between parentheses (Ps, *Pinus sylvestris*; Pn, *Pinus nigra*; Ls, *Larix sibirica*).

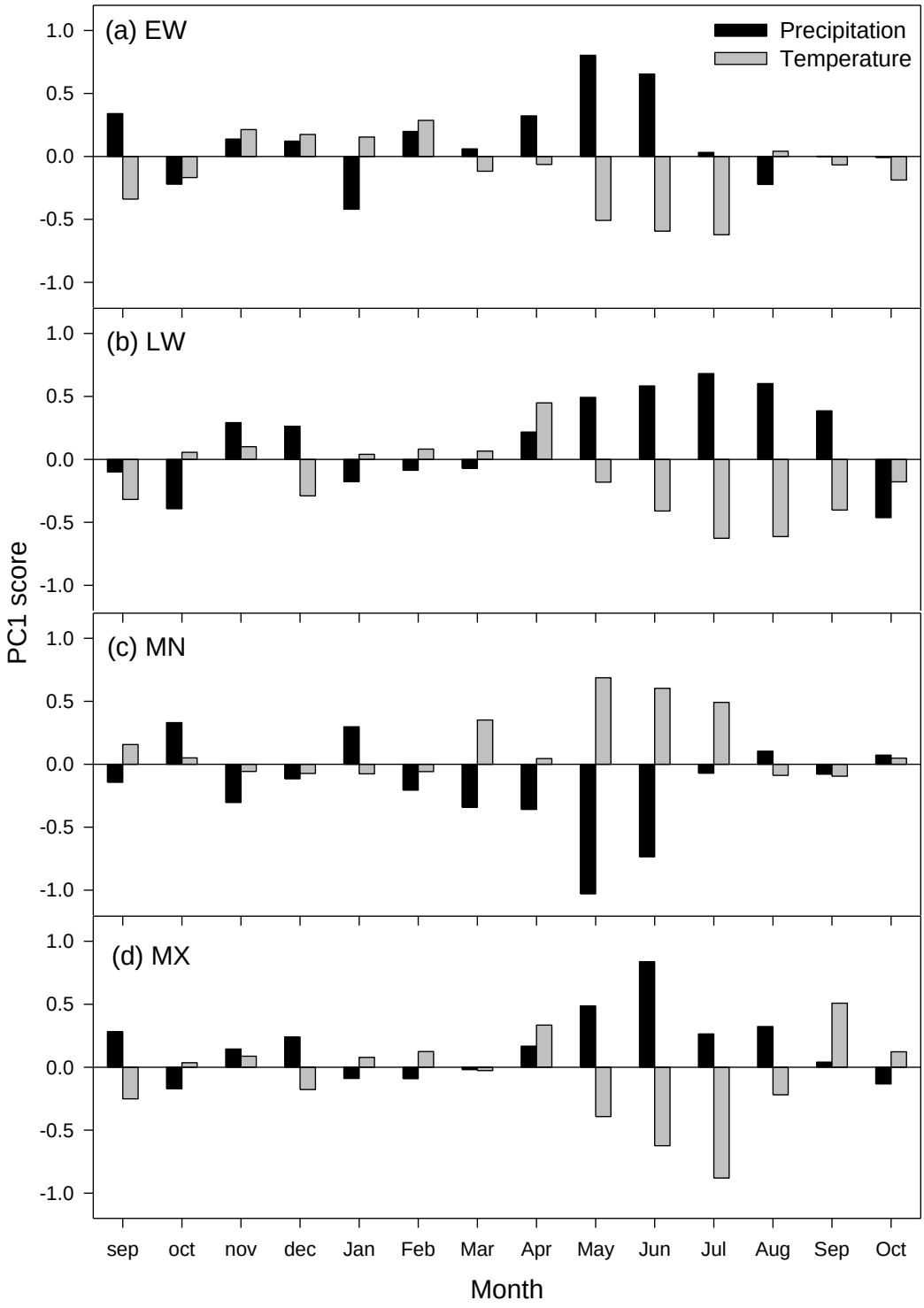

Figure 4. Scores of the first principal component (PC1) of Principal Component Analyses calculated on the indices of earlywood (a, EW) and latewood width (b, LW) data and minimum (c, MN) and maximum (d, MX) wood density data. Scores are presented for the correlations of tree-ring variables with monthly precipitation (black bars) and temperature (grey bars) data corresponding to September prior to tree-ring formation up to October (previous- and current-year months are abbreviated by lowercase and uppercase letters, respectively).

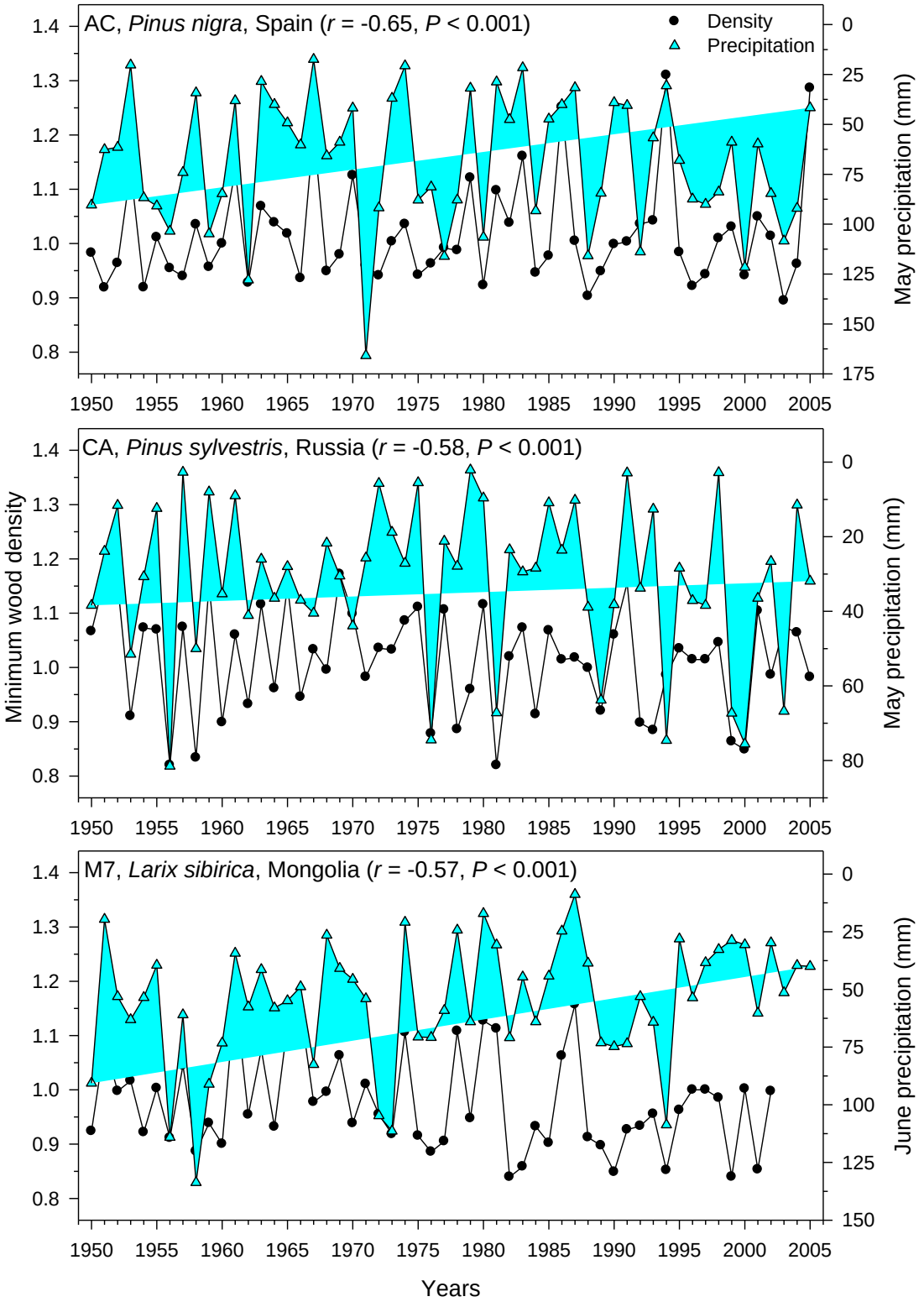

Figure 5. Main relationships observed between climate variables (May and June precipitation) and the indexed series of minimum wood density in each country. In each plot the correlation between precipitation and wood density values are shown with their corresponding significance levels (*P*). Note the reverse precipitation scales. See sites' codes in Table 1.

Supporting Information

				Precipitation														Mean temperature											
				Previous year				Current year										Previous year				Current year									
Country	**Site**	**Species**	**Variable**	**sep**	**oct**	**nov**	**dec**	**Jan**	**Feb**	**Mar**	**Apr**	**May**	**Jun**	**Jul**	**Aug**	**Sep**	**Oct**	**sep**	**oct**	**nov**	**dec**	**Jan**	**Feb**	**Mar**	**Apr**	**May**	**Jun**	**Jul**	**Aug**	**Sep**	**Oct**
Spain	PN	Ps	EW	0.16	-0.24	-0.01	0.03	-0.29	0.04	-0.03	-0.16	0.05	0.12	0.10	-0.08	-0.11	0.06	-0.15	0.12	0.01	-0.33	-0.24	-0.05	-0.32	0.11	0.34	-0.01	-0.23	-0.18	0.01	-0.12
	LR			0.03	-0.22	0.12	0.18	-0.07	0.19	0.27	0.09	**0.56**	0.11	0.11	-0.26	-0.07	0.13	0.06	-0.13	0.09	0.16	0.06	0.14	-0.23	0.03	-0.14	-0.14	-0.21	0.12	0.02	-0.18
	LR	Pn		0.13	-0.19	0.13	0.20	0.12	0.01	0.04	0.03	**0.44**	0.30	0.10	-0.08	-0.12	0.08	-0.13	-0.08	0.10	0.20	0.07	0.35	0.01	0.13	-0.03	-0.11	-0.31	0.09	0.07	-0.14
	AC			0.32	-0.10	0.21	0.28	0.11	0.13	0.19	0.17	**0.57**	0.24	0.16	-0.02	-0.17	-0.06	-0.01	-0.06	0.00	0.05	0.01	0.17	-0.12	-0.07	-0.26	-0.12	-0.33	-0.03	0.10	-0.15
Russia	CA	Ps		-0.12	0.22	0.04	0.06	-0.06	-0.05	0.16	-0.09	0.27	-0.02	-0.29	0.02	0.15	0.19	0.12	0.06	0.21	0.22	0.21	0.30	0.26	0.06	**-0.48**	**-0.53**	0.13	0.03	-0.08	-0.06
	EF	Ls		0.21	0.00	0.14	-0.23	**-0.50**	-0.03	-0.08	0.03	-0.04	0.12	-0.11	-0.17	0.05	-0.12	-0.28	-0.09	0.15	0.10	0.04	-0.11	0.13	0.06	-0.18	-0.20	0.05	0.27	-0.03	-0.01
	KH			0.33	0.03	0.14	-0.21	-0.35	0.06	-0.08	0.28	0.11	0.05	-0.20	-0.18	0.14	-0.15	-0.35	-0.05	0.07	-0.01	0.02	0.08	0.08	0.08	-0.29	-0.23	-0.02	0.07	-0.07	-0.10
Mongolia	M0	Ls		0.10	-0.10	-0.08	-0.05	-0.23	-0.01	-0.28	0.15	-0.06	**0.47**	-0.01	0.11	0.14	0.07	-0.25	-0.12	0.10	-0.04	0.07	-0.26	-0.13	-0.09	0.03	-0.16	**-0.43**	-0.12	-0.17	0.06
	M7			-0.01	0.01	-0.21	-0.03	-0.31	0.20	-0.09	0.29	0.23	**0.55**	0.13	0.05	0.15	-0.07	-0.12	0.04	0.08	0.02	0.15	0.11	0.01	-0.24	-0.19	-0.28	-0.31	-0.09	-0.06	0.19
Spain	PN	Ps	LW	-0.14	-0.24	0.20	0.12	-0.06	-0.08	-0.08	0.02	0.08	0.23	0.24	0.36	0.16	-0.17	-0.24	0.17	0.26	-0.15	-0.04	0.06	0.03	**0.42**	0.26	-0.02	-0.17	-0.26	-0.11	-0.05
	LR			-0.17	-0.12	0.16	0.23	-0.01	-0.03	0.07	0.08	0.26	0.10	0.36	0.35	0.23	-0.23	-0.03	0.05	0.01	-0.17	0.05	-0.01	-0.02	0.27	-0.06	-0.11	-0.23	-0.37	-0.22	-0.14
	LR	Pn		-0.16	-0.21	0.21	0.24	0.12	-0.07	0.00	0.07	0.25	0.13	0.34	0.42	0.20	-0.22	-0.12	0.02	0.02	-0.12	0.04	0.07	0.09	0.26	-0.03	-0.09	-0.25	-0.31	-0.17	-0.14
	AC			0.07	-0.18	0.22	0.34	0.07	0.03	0.08	0.22	0.27	0.27	**0.43**	0.23	0.18	-0.19	0.07	0.02	0.04	-0.11	0.08	0.10	0.02	0.16	-0.05	-0.01	-0.17	-0.22	-0.08	-0.14
Russia	CA	Ps		0.20	-0.08	0.30	-0.21	-0.03	-0.23	0.07	-0.22	0.40	0.01	-0.06	0.05	0.11	0.03	-0.09	-0.02	-0.09	-0.11	-0.02	-0.01	0.02	-0.08	**-0.44**	-0.35	-0.22	-0.09	-0.18	-0.05
	EF	Ls		0.20	0.00	0.14	-0.23	**-0.50**	-0.03	-0.08	0.02	-0.04	0.13	-0.09	-0.17	0.06	-0.11	-0.28	-0.09	0.17	0.09	0.04	-0.12	0.14	0.04	-0.19	-0.20	0.03	0.28	-0.03	-0.02
	KH			0.29	-0.04	-0.02	-0.08	-0.29	-0.02	-0.12	0.10	0.08	0.34	-0.02	-0.12	-0.01	-0.10	-0.25	-0.03	0.15	0.00	0.04	0.10	0.12	0.21	-0.26	-0.16	-0.10	-0.08	-0.01	0.06
Mongolia	M0	Ls		0.09	-0.02	-0.03	-0.08	-0.22	0.08	-0.10	0.18	-0.06	0.36	0.16	0.12	0.17	-0.07	-0.05	0.11	0.10	0.04	0.06	-0.02	-0.05	0.03	0.06	-0.25	-0.25	0.19	-0.16	0.20
	M7			0.07	0.04	-0.18	-0.07	-0.23	0.20	-0.08	0.27	0.23	**0.56**	0.34	0.11	0.12	-0.08	-0.15	-0.05	-0.06	0.05	0.05	0.08	0.13	-0.06	-0.16	-0.32	-0.31	-0.10	-0.07	0.13

				Precipitation														Mean temperature											
				Previous year				Current year										Previous year				Current year									
Country	**Site**	**Species**	**Variable**	**sep**	**oct**	**nov**	**dec**	**Jan**	**Feb**	**Mar**	**Apr**	**May**	**Jun**	**Jul**	**Aug**	**Sep**	**Oct**	**sep**	**oct**	**nov**	**dec**	**Jan**	**Feb**	**Mar**	**Apr**	**May**	**Jun**	**Jul**	**Aug**	**Sep**	**Oct**
Spain	PN	Ps	MN	-0.05	0.21	-0.17	-0.01	0.21	-0.17	-0.28	-0.05	-0.02	-0.36	-0.28	0.05	-0.07	0.08	-0.06	-0.13	-0.14	0.14	0.06	0.07	0.32	-0.04	-0.04	-0.03	-0.09	0.11	0.13	0.04
	LR			0.04	0.31	-0.17	-0.19	-0.03	-0.23	-0.36	-0.18	**-0.54**	-0.30	-0.14	0.12	-0.06	-0.01	-0.09	0.06	-0.11	-0.08	-0.14	0.01	0.26	-0.02	0.21	0.08	0.05	-0.05	0.19	0.10
	LR	Pn		-0.02	0.24	-0.11	-0.17	-0.08	-0.08	-0.22	-0.09	**-0.52**	-0.32	-0.15	0.03	0.03	-0.14	0.04	0.05	-0.17	-0.09	-0.10	-0.20	0.28	-0.11	0.13	0.18	0.17	-0.06	0.07	0.16
	AC			-0.21	0.15	-0.25	-0.28	-0.25	-0.02	-0.26	-0.21	**-0.65**	-0.25	-0.15	-0.08	0.18	0.05	0.02	0.01	-0.10	-0.08	-0.05	-0.12	0.16	-0.07	0.29	0.24	0.33	0.10	0.00	0.17
Russia	CA	Ps		0.13	-0.17	0.05	-0.12	0.03	0.02	-0.10	0.05	**-0.58**	-0.16	-0.04	-0.08	-0.26	0.03	-0.16	-0.17	0.21	-0.10	-0.16	-0.13	0.09	0.11	**0.45**	0.21	0.17	-0.26	0.27	0.10
	EF	Ls		-0.18	0.08	-0.16	0.06	0.44	0.05	0.03	-0.18	**-0.47**	-0.16	-0.01	0.14	0.02	0.01	0.25	0.11	-0.12	-0.02	0.03	-0.01	-0.31	-0.11	0.17	0.30	0.11	-0.29	0.03	-0.02
	KH			-0.26	-0.06	-0.18	0.13	0.42	0.02	0.02	-0.35	**-0.40**	0.00	0.13	0.02	-0.09	0.17	0.33	-0.04	0.07	-0.07	0.06	0.11	0.15	-0.07	0.21	0.34	0.05	-0.09	0.05	0.00
Mongolia	M0	Ls		-0.04	0.11	0.01	0.28	0.25	-0.15	0.17	-0.08	-0.18	**-0.52**	0.06	-0.01	-0.16	-0.01	0.05	0.02	0.19	-0.10	-0.02	0.01	0.00	0.14	0.13	0.10	0.27	-0.03	-0.14	-0.37
	M7			-0.06	-0.20	-0.08	0.09	0.20	-0.29	0.00	-0.16	-0.11	**-0.57**	0.26	-0.04	-0.22	-0.10	-0.02	-0.03	-0.10	0.09	0.01	0.02	0.28	0.20	0.27	0.21	0.14	0.04	-0.01	-0.26
Spain	PN	Ps	MX	0.16	0.17	-0.14	-0.37	-0.13	-0.09	-0.21	-0.27	-0.22	0.19	**-0.49**	-0.31	-0.36	0.05	0.07	0.00	0.12	0.23	0.10	0.23	0.05	0.07	0.18	0.11	0.10	0.35	**0.39**	0.21
	LR			-0.07	-0.07	0.09	0.13	0.14	-0.11	0.03	0.04	0.22	0.32	0.15	0.22	-0.05	-0.06	-0.05	0.10	0.11	-0.04	0.15	0.06	-0.07	0.26	-0.11	-0.21	**-0.57**	-0.32	-0.10	-0.03
	LR	Pn		0.17	0.00	0.08	0.11	0.17	-0.25	-0.16	-0.11	0.17	**0.42**	-0.01	0.09	-0.15	0.06	-0.10	0.15	0.09	0.08	0.04	0.29	0.13	0.31	0.02	-0.09	**-0.51**	-0.13	0.20	0.09
	AC			0.25	-0.18	0.20	0.25	0.17	-0.02	0.18	0.22	0.32	0.37	0.19	0.18	-0.12	-0.07	0.08	0.11	0.06	-0.15	-0.04	0.10	-0.15	0.14	-0.13	-0.18	**-0.45**	-0.21	0.11	-0.20
Russia	CA	Ps		-0.02	0.07	-0.13	0.09	-0.04	0.04	-0.11	-0.11	0.17	0.01	0.02	0.05	0.19	-0.03	-0.15	-0.08	-0.16	0.07	-0.08	0.06	0.12	0.02	-0.19	**-0.43**	-0.10	-0.02	-0.07	-0.03
	EF	Ls		0.21	0.11	0.14	-0.10	-0.35	0.04	0.05	0.01	0.04	0.26	0.05	-0.07	0.03	-0.04	-0.19	-0.16	-0.07	-0.06	0.02	-0.07	0.16	0.16	-0.19	-0.26	-0.13	0.15	0.04	0.09
	KH			0.23	0.04	0.05	-0.08	-0.28	0.06	-0.06	0.18	0.18	0.29	-0.02	-0.02	0.05	-0.13	-0.19	-0.04	-0.02	-0.12	0.08	0.07	0.10	0.18	-0.32	-0.22	-0.32	-0.01	0.00	0.10
Mongolia	M0	Ls		0.00	-0.31	-0.03	0.02	-0.05	-0.05	-0.01	0.00	-0.20	0.11	-0.36	0.37	0.14	0.01	-0.26	-0.08	0.20	0.23	-0.13	-0.26	-0.19	0.05	0.07	-0.02	-0.03	0.11	-0.16	-0.02
	M7			0.16	-0.09	-0.12	0.00	-0.27	0.08	-0.11	0.02	0.12	**0.60**	0.08	0.15	0.15	-0.01	-0.12	-0.08	0.15	-0.03	0.09	-0.01	-0.06	-0.08	-0.11	-0.35	-0.37	-0.06	-0.17	0.32

Table S1. Correlations (Pearson coefficients) calculated by relating monthly climatic variables (precipitation, mean temperature) and indexed tree-ring variables (EW, earlywood width; LW, latewood width; MN, minimum density; MX, maximum density) considering the common 1950-2002 period. Data correspond to the nine study sites sampled at three countries (Spain, Russia and Mongolia) and corresponding to three conifer species (Ps, *Pinus sylvestris*; Pn, *Pinus nigra*; Ls, *Larix sibirica*). Correlations were calculated from September prior to tree-ring formation up to October (previous- and current-year months are abbreviated by lowercase and uppercase letters, respectively). Cells with grey background indicate correlations significant at the 0.05 level, and bold values indicate $P < 0.01$.

Supporting Information

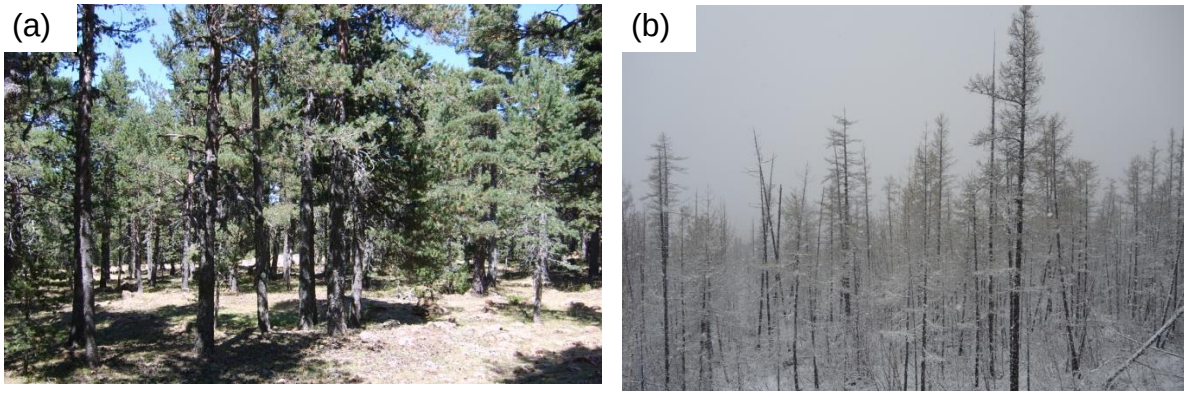

Figure S1. Images of two study sites situated in Spain (a, Peñarroya, *Pinus sylvestris* forest in summer) and Russia (b, Shira, *Larix sibirica* forest in winter).

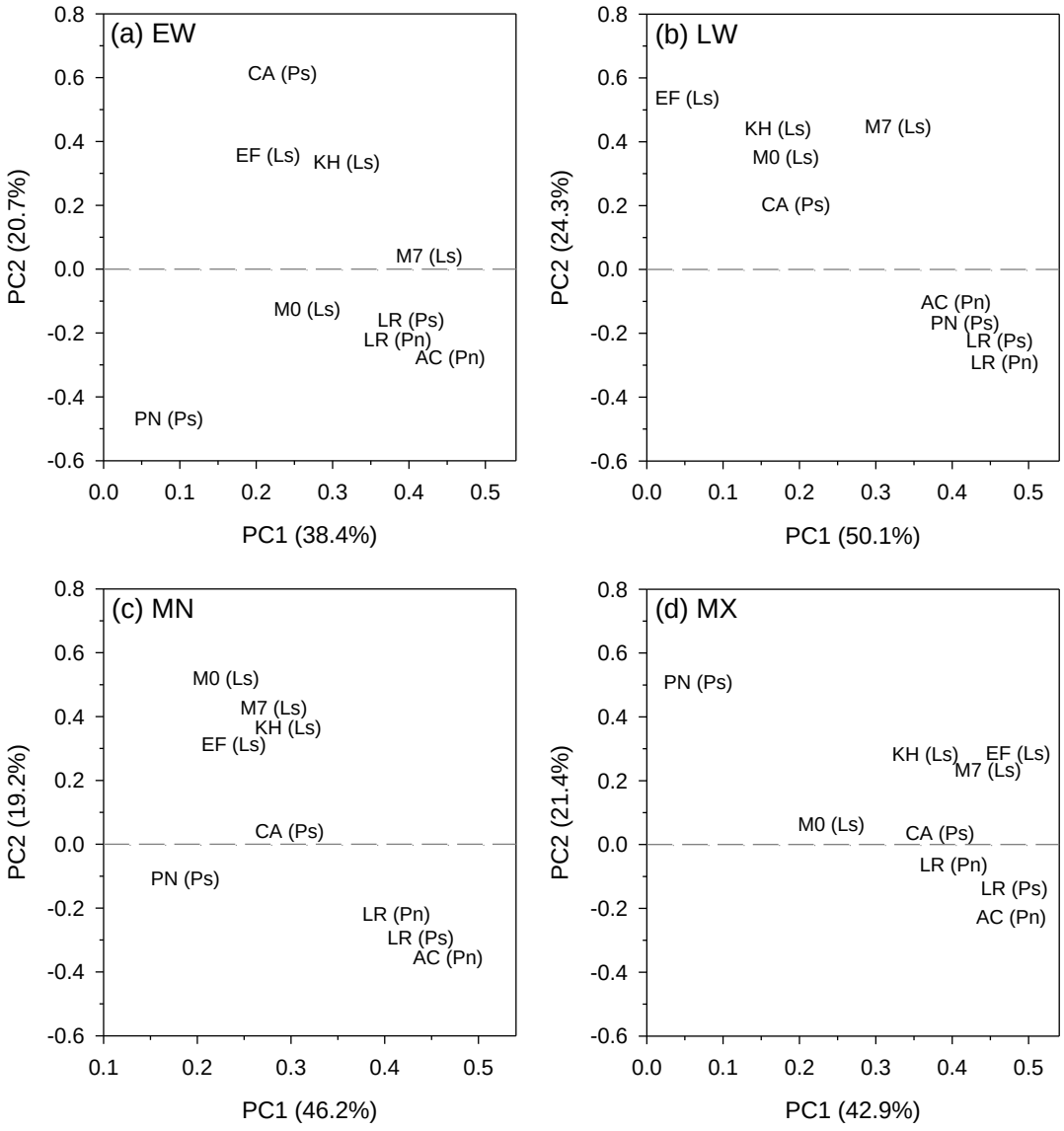

Figure S2. Scatters showing the scores of the first (PC1) and second (PC2) principal components obtained by calculating Principal Component Analyses on the variance-covariance matrices of climate-growth or climate-density (seasonal width and density data) correlations. The graphs correspond to earlywood (a, EW) and latewood (b, LW) width indices and minimum (c, MN) and maximum (d, MX) wood densities. Correlations were calculated for the common 1950-2002 period. The sites are abbreviated by two-letter codes as in Table 1 followed by species abbreviations between parentheses (Ps, *Pinus sylvestris*; Pn, *Pinus nigra*; Ls, *Larix sibirica*). The percentages of variance accounted for by PC1 and PC2 are indicated in each graph.